Viscoelastic granular dampers under low amplitude vibration

B Darabi[1], J A Rongong[2] and T Zhang[2]

[1] Department of Mechanical Engineering, Islamic Azad University Central Tehran Branch, Iran.

[2] Department of Mechanical Engineering, The University of Sheffield, UK.

Corresponding Author

Jem A Rongong

The University of Sheffield, Department of Mechanical Engineering, Mappin Building, Mappin Street, Sheffield, S1 3JD, UK.

j.a.rongong@sheffield.ac.uk

Abstract

This paper considers dampers comprising collections of viscoelastic particles that are subjected to vibrations whose amplitude is such that slip between particles is negligible. Energy dissipation occurs primarily by viscoelastic processes within each particle and is maximised when standing waves are set up in the granular medium. In this work, the medium is represented as an equivalent viscoelastic solid and predictions of performance employ models constructed using standard finite element software. Two numerical approaches are considered: one uses the Direct Frequency Response and the other uses standard modal analysis in conjunction with analytical expressions for energy dissipation based on the wave equation. The performance of these prediction techniques is compared with measured behaviour from experiments on a box-shaped structure and a hollow composite tube assembly. The computational efficiency of the modal technique allowed a brief investigation of the effects of uncertainties in the actual nature of the granular arrangement. Results show that both prediction methods give a reasonable level of accuracy. Differences between predicted and measured behaviour are shown to be of the same order as the uncertainty in the prediction itself. For the systems considered, it is shown that the methods are appropriate for acceleration amplitudes up to almost that of gravity.

Keywords

Damping, viscoelastic, granular, particle damper, hollow structure, uncertainty

1 Introduction

When a granular medium is subjected to vibration, energy is dissipated through inelastic deformation and friction between individual particles. If the granular medium is placed in a cavity that is integral to or attached to a vibrating structure, it can provide useful levels of damping. Performance depends on many parameters including vibration frequency and amplitude.

One type of granular damper that has been studied extensively is the particle damper. Here the particles are small and hard, often metallic or ceramic, and the important energy dissipation mechanisms are friction and inelastic losses at the interface. This type of granular system, is not discussed here. Instead, this paper considers the damping obtained from granular systems where loss of contact or slip between particles is rare and damping arises from energy dissipation within the particle. Under such conditions, it has been shown that a granular medium consisting of relatively large and flexible polymeric spheres can provide very high levels of structural damping. This occurs for vibration modes of the host structure that occur in frequency ranges where standing waves are present within the granular medium. Under these conditions, excitation of the host structure leads to significant interaction with the vibration modes within the granular medium which act in a similar way to tuned mass dampers.

Granular dampers employing standing waves in a collection of viscoelastic particles were first described publicly in a patent application by House and Hilliar (1990). Subsequently experimental studies were used to demonstrate the effectiveness of the method on hollow beams (Oyadiji, 1996; Pamley et al, 2001; Rongong and Tomlinson, 2002). Theoretical methods, based on representing the granular medium as an equivalent solid, have been used to provide estimates of modal damping (Pamley et al, 2001; Rongong and Tomlinson, 2002) and frequency response (Varanasi and Nayfeh) of hollow beams. These analyses were inspired by the original work of Ungar and Kerwin (1964) who derived expressions for the energy loss in thick viscoelastic layers bonded to metal plates.

At very high levels of excitation, even for highly damped soft particles, the equivalent solid assumption becomes invalid. The amplitude at which particles begin to separate is related to the ratio of vibration acceleration to gravitational acceleration. It has been shown that separation first starts to occur under conditions where an internal resonance occurs in the granular medium and the location of the separation is at the maximum deflection point of the internal wave (Poschel et al 2000). For motion parallel to gravity, separation can occur when the acceleration ratio is less than unity.

Numerical studies involving the Discrete Element Method have also been carried out for granular dampers consisting of soft, high loss particles (Darabi and Rongong, 2012). In this approach, the properties of individual particles (including mass, complex stiffness and friction) were defined and the energy dissipation estimated for large collections of these particles subjected to prescribed vibration. While this type of analysis gives considerable insight into the effects of individual parameters affecting performance, it is not suitable for optimisation of engineering structures containing granular dampers

because of the high computational cost involved. There is currently need for a prediction method for viscoelastic granular dampers that is compatible with large finite element models of irregular structures.

This aim of this paper is to develop and evaluate approaches that are appropriate for high loss particles subjected at low amplitude vibrations (where inter-particle separation and slip are minimal) and energy dissipation is dominated by viscoelastic losses in the particles. These approaches provide predictions of energy loss in the medium and the resulting frequency response of the damped host structure. As the prediction methods model the granular medium as an equivalent viscoelastic solid, the paper considers the limits of applicability of such an approximation as the amplitude increases.

2 Methodology and Objectives

The focus of this work was to develop straightforward approaches for predicting the performance of granular dampers in engineering structures at low amplitude using computational resources normally available to practising engineers. The fundamental assumption used was that at low vibration levels, the majority of the particles would not separate and therefore their behaviour could be represented by a viscoelastic solid. While a procedure that couples the vibration of the flexible host structure to a viscoelastic discrete element code is likely to provide a more physically representative (and therefore possibly more general) solution, such tools are currently not widely available and the computational cost would be prohibitively high for design optimisation studies. Instead, the approach taken was to provide closed-form equations that can be used alongside standard finite element analysis procedures.

The work presented here uses one granular system involving relatively large spheres made of an elastomeric material. Experimental and numerical studies are carried out when granules are used to fill two different types of structure: a rigid box and a hollow cylindrical beam. The similarity between the experimental and numerical results is used to validate the prediction procedures discussed in the paper. While, in the studies carried out, excitation is applied in a direction perpendicular to gravity, significant differences in results for excitation in other directions are not expected as the vibration amplitude remains small.

The finite element models employed, for both the equivalent viscoelastic solid and the host structure, were constructed using quadratic brick elements with reduced integration. The mesh density was set in each direction such that there were at least 8 elements to approximate the shortest wavelengths considered. While in this work the commercial software Abaqus was used, any other code that could run elastic natural frequency extraction routines and frequency domain forced vibration analysis would have given the same results.

The paper is structured around the need to achieve four principal objectives which are described briefly below.

1. To obtain properties of an equivalent viscoelastic solid from tests on the bulk material from which the granules are made. This includes efforts to account for uncertainty arising from the variable nature of typical granular arrangements and is discussed in Section 3.
2. To evaluate methods to predict the energy dissipation within a granular medium subjected to low amplitude vibration. This is carried out using a rigid box filled with viscoelastic particles and is presented in Section 4.
3. To develop and validate methods for predicting the damped frequency response of structures that are more complicated than rectangular beams. This activity is described in Section 5, where a composite tube with heavy metal end caps is subjected to transverse vibrations.
4. To explore the limits to which predictions based on the equivalent solid approximation are valid. This was investigated experimentally by altering the vibration amplitude of the composite tube assembly and is described in Section 6.

3 Equivalent viscoelastic solid

As the vibration amplitude considered in this work is relatively low, it was possible to consider the granular medium as an equivalent viscoelastic solid. This is an important simplification as it allows predictions to be made using standard finite element software. For consistency, the granular medium considered here was composed of nominally identical spheres (each 15.1 mm in diameter) made from an elastomeric polymer selected to have its transition zone near room temperature. The procedure undertaken to obtain equivalent properties is described here including efforts to account for uncertainties arising from the precise nature of the granular arrangement.

3.1 Viscoelastic behaviour

As this work concentrated on frequency domain behaviour, the complex modulus approach was considered adequate. This is written as,

$$E^{*} = E_{v}\left(1 + j\eta_{v}\right) \tag{1}$$

where E_v is the elastic modulus, η_v is the loss factor and $j = \sqrt{-1}$. Note that causality is satisfied if the loss factor tends to zero at low frequency.

For the polymeric material used, information regarding the temperature and frequency dependence of the complex modulus was condensed into its viscoelastic master curve. This curve was constructed by applying the temperature-frequency superposition principle (Ferry, 1980) to measured data obtained using Dynamic Mechanical Thermal Analysis (DMTA) equipment. The method assumes that the modulus and loss factor at temperature T can be obtained from known frequency dependent properties at a reference temperature T_r by multiplying the frequency scale by a shift factor α that is specific for

that material at that particular temperature. To account for the increase in stored energy with temperature, and additional scaling is required for the elastic modulus such that,

$$E_v = E_r \frac{T}{T_r} \tag{2}$$

where E_r is sometimes referred to as the reduced modulus. Thus the complex modulus at any temperature and frequency can be recovered if curves defining the reduced modulus and loss factor against frequency are constructed and a suitable curve linking temperature and frequency shift is specified.

For the material considered here, a cuboid specimen (11.5×4.5×3.5 mm) was cut from one of the polymer spheres. It was bonded between two parallel plates on the DMTA machine, as shown in Figure 1, and excited in a tension-compression mode. The upper plate was controlled to move sinusoidally with amplitude 9.2 μm and the resulting force signal was used to find the complex stiffness of the specimen and hence the Young's modulus and the loss factor for the material. Characterisation was carried out at a number of frequencies between 1 and 30 Hz over a temperature range −60 to 60 °C.

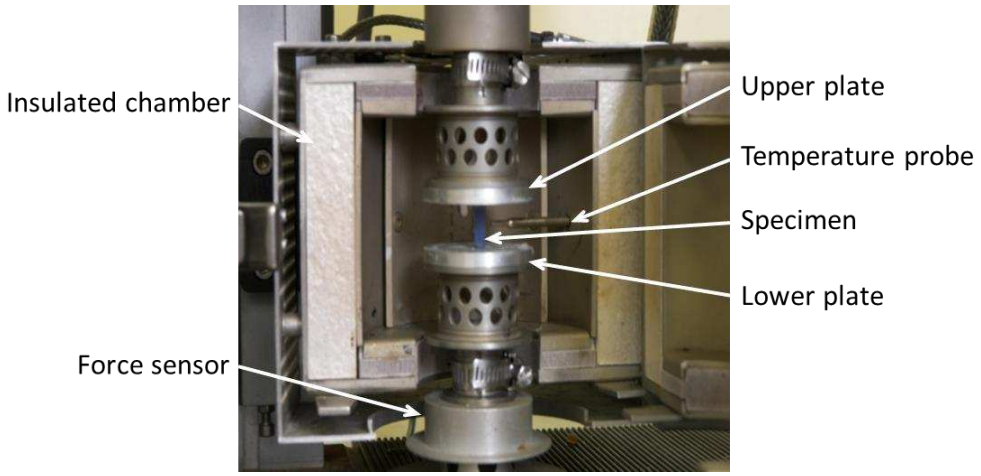

Figure 1: DMTA characterisation of polymer specimen using Metravib VA2000 equipment

The frequency dependent reduced modulus and loss factor curves were obtained at a reference temperature $T_r = -17\,°C$, by defining and optimising the shift factor for each temperature. The optimisation routine used the Differential Evolution algorithm and aimed to minimise the distance from individual data points to smooth, spline-based curves. The resulting curves are presented in tabular form in Table 1. The quality of fit of individual points to the master curves can be seen in Figure 2 from which it can be concluded that there is relatively low scatter.

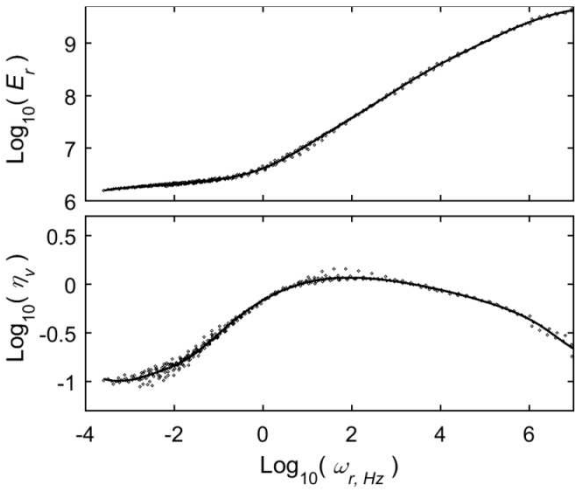

Figure 2: Fit of individual data points to complex modulus curves presented in Table 1

Note that to recover properties at a desired frequency ω_{Hz} and temperature T, first the reduced frequency should be found by applying the correct frequency shift. The shift factor for the desired temperature is found by interpolation of the shift curve in Table 1. Thus,

$$\log_{10}(\omega_{\mathrm{r,Hz}}) = \log_{10}(\omega_{\mathrm{Hz}}) + \log_{10}(\alpha) \tag{3}$$

Reduced modulus and loss factor are be obtained by interpolation of the complex modulus curve in Table 2 after which the actual elastic modulus is calculated using Equation 2.

Table 1: Viscoelastic properties of polymeric material

Frequency / temperature shift curve			Complex modulus curve		
T , °C	$\log_{10}(\alpha)$		$\log_{10}(\omega_{\mathrm{r,Hz}})$	$\log_{10}(\mathrm{E_r})$	$\log_{10}(\eta_{\mathrm{v}})$
-60	5.2330		-3.5848	6.2017	-0.9705
-52	3.9814		-2.8585	6.2685	-0.9676
-44	2.8592		-2.1321	6.3142	-0.8590
-36	1.8582		-1.4058	6.3697	-0.6662
-28	0.9706		-0.6795	6.4574	-0.3819
-20	0.1884		0.0468	6.6348	-0.1520
-12	-0.4964		0.7731	6.9456	-0.0079
-4	-1.0916		1.4994	7.3179	0.0604
4	-1.6052		2.2258	7.6934	0.0667
12	-2.0453		2.9521	8.0797	0.0344
20	-2.4196		3.6784	8.4526	-0.0234
28	-2.7363		4.4047	8.7777	-0.0992
36	-3.0032		5.1310	9.0769	-0.1943
44	-3.2283		5.8574	9.3519	-0.3230
52	-3.4195		6.5837	9.5541	-0.5264
60	-3.5848		7.3100	9.6743	-0.7055

3.2 Equivalent properties for a granular system

The average density of a granular system is,

$$\rho = \rho_v \phi \tag{4}$$

where ρ_v is the mean density of each particle and ϕ is the packing fraction. As the energy dissipation contribution of inter-particle friction is ignored, the loss factor for the equivalent solid can be assumed to be the same as the loss factor for the original viscoelastic material, hence,

$$\eta = \eta_v \tag{5}$$

The effective Young's modulus and Poisson's ratio of a granular system are known to be much lower than that of the bulk material. The approach taken in this paper was to use expressions for an equivalent solid based on randomly packed identical spheres derived by Walton (1987). For rough spheres subjected to an applied hydrostatic pressure p, the effective Poisson's ratio for the equivalent solid ν is given by,

$$\nu = \frac{\nu_v}{2(5-3\nu_v)} \tag{6}$$

and the associated Young's modulus,

$$\mathrm{E} = \frac{1-2\nu}{2}\left(\frac{3\mathrm{E_v}^2\phi^2\mathrm{N}^2\mathrm{p}}{\pi^2(1-\nu^2)}\right)^{\frac{1}{3}} \tag{7}$$

where ν_v and $\mathrm{E_v}$ are the Poisson's ratio and the elastic part of the Young's modulus of the material that the spheres are formed of, and N the average number of contact points per particle (the coordination number). From Equation 7 it can be seen that in addition to the properties of the polymer material itself, there are three parameters that control behaviour: the packing fraction, the coordination number and the confining pressure. These are discussed briefly in the following sections.

Packing fraction and coordination number

The specific way in which the particles are ordered within a cavity affects the packing ratio and the coordination number. For regular arrangements, this can be calculated theoretically: for example, a face-centred cubic (FCC) arrangement has a packing factor $\phi = 0.74$ and coordination number $\mathrm{N} = 12$ while for a cubic arrangement $\phi = 0.524$ and $\mathrm{N} = 6$. Random arrangements have been studied numerically and experimentally by many researchers (Iwata and Homma, 1974; Nolan and Kavanagh, 1992; Zamponi, 2008). It has been shown that packing is affected by factors such as friction, applied pressure and size ratio between particle and container. Quoted values for mono-sized, randomly packed spheres typically occur in the ranges $\phi = 0.52$ to 0.64 and $\mathrm{N} = 4$ to 6.

Confining pressure

In a cavity filled with particles, even under static conditions, the pressure (and hence the deflection) varies with depth because of gravity loading. The granular system redirects some of the load to the cavity walls so that the pressure in a deep fill is less than would be in an equivalent fluid. One of the earliest models linking pressure to depth was provided by Janssen (1895) and the subject has remained an active area of research since. For the purposes of this work, Janssen's approach was considered adequate to provide the confining pressure (in Equation 7) and therefore,

$$p = \frac{\rho g}{\chi S}(1 - e^{-\chi S h_g}) \tag{8}$$

where g is the acceleration due to gravity, h_g is the depth in the direction of gravity, and χ is an empirical load redirection factor that depends on the granular medium itself. S is the shape factor of the container and is the ratio of the perimeter to the area of the container cross-section perpendicular to gravity.

3.3 Specification of parameters

The equations in Section 3.2 show that even with considerable simplification, there remain a significant number of parameters required to obtain an equivalent solid model. As some of these can vary depending of the exact nature of the packing and others are not straightforward to measure exactly, an attempt was made to take into account the resulting uncertainty. The field of uncertainty quantification is extensive but is not discussed in detail here. Instead, a brief justification is provided for the approach employed. From the literature and qualitative observations, it was clear that the parameters affecting the arrangement of particles lie within typical ranges with more results near the mean value and a relatively small number of outliers. For this reason the distribution was assumed Gaussian and the range of values based on ± 2 standard deviations (approximately 95% of all results). Uncertainty was then accounted for using 1000 different simulations with parameters selected randomly assuming a Gaussian distribution. Alternatives to this approach would be to assume random distribution within a range whose endpoints are uncertain, or to approach the problem from an info-gap theory perspective (Ben-Haim, 2001). However, as the purpose of this exercise was to help judge the accuracy of modelling approaches against inherent variability in the system rather than a dedicated evaluation of uncertainty, the method used was considered adequate. Values selected for parameters are given in Table 2.

Table 2: Parameters used to define the granular material

Parameter	Symbol	Mean value	Standard deviation
Packing ratio	ϕ	0.58	0.03
Coordination number	N	6	1
Redirection factor	κ	0.65	0.075
Friction coefficient	μ	1	0.1
Temperature, °C	T	22	2
Gravity, m/s^2	g	9.81	0
Density of polymer, kg/m^3	ρ_v	1170	0

It can be seen in Table 2 that the temperature is also taken as a variable parameter. While this is not a specific property of the granular medium, the properties of the viscoelastic material were very sensitive to temperature it and it was not possible to define it more precisely in the laboratory conditions. Other parameters including dimensions were given crisp values. It was assumed that the ranges considered for coordination number and packing fraction would account for variations in the depth caused by the randomness of the particle locations.

4 Energy dissipation

This section reports a comparison between experimentally measured and numerically predicted energy dissipation provided by a granular medium. In this study, the viscoelastic spheres discussed in Section 2 were placed in an open sided box and vibrated perpendicular to gravity over a relatively wide frequency range at low overall amplitude. The test configuration was the same as used elsewhere to characterise moderately low frequency, high amplitude damping in granular systems (Darabi and Rongong, 2012). The suspension arrangement minimises energy losses from sources other than the granular material.

4.1 Rigid box

The open-sided box was constructed using polymethyl methacrylate (PMMA) blocks, each of thickness 30 mm, to create a cavity with dimensions 180×120×40 mm. The box was suspended with the open side facing upwards using supports with sufficient flexibility to approximate free boundary conditions. Excitation was applied horizontally in line with the longest dimension of the cavity as shown in Figure 3.

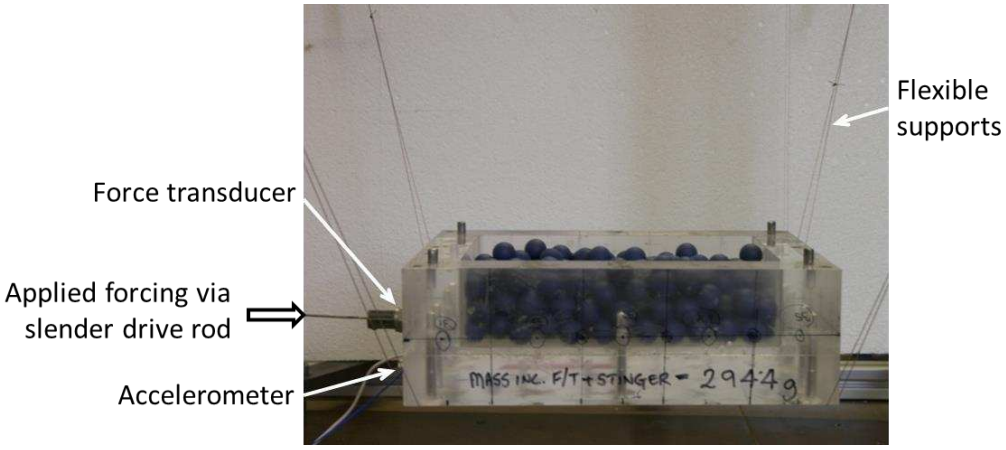

Figure 3: Rigid box configuration

The design of the box ensured that its fundamental resonance was much higher than the frequency range of interest for this study (between 10 and 400 Hz). This allowed investigation of the performance of the granular medium itself as the vibration of the boundaries did not change with position. Additionally, as the box was shallow and had an open face, the level of confinement experienced by the particles was relatively low.

4.2 Physical experiment

The box was suspended using nylon line and light metal springs in series. The suspension modes were found to occur at frequencies below 5 Hz. Sinusoidal excitation was provided via an electrodynamic exciter attached to one end of the box through a slender drive rod. The applied force was measured with a piezoelectric transducer and the acceleration near the excitation point measured with a small piezoelectric accelerometer. Force and acceleration signals were obtained for excitation amplitudes of 10, 1 and 0.1 μm over a range of frequencies between 10 and 400 Hz. The experiment was first conducted with the container empty in order to find the phase error due to the boundary conditions and electronics. This error, although relatively small (5% at 350 Hz), was subtracted from measurement to provide the corrected contribution of the granular medium. The container was filled with 260 randomly placed particles and tests repeated. The dissipated power was obtained from,

$$\mathrm{P}_{\mathrm{real}} = \frac{1}{2} |\mathrm{F}||\mathrm{V}| \cos\left(\theta_{\mathrm{F}} - \theta_{\mathrm{V}}\right) \tag{9}$$

where F and θ_{F} are respectively the amplitude and corrected phase angle of the force signal and V and θ_{V} the amplitude and corrected phase angle of the velocity. Note that the frequency domain velocity information was obtained from the Fourier Transform of accelerometer readings divided by $\mathrm{j}\omega$ where ω is the excitation frequency in radians/second. The power dissipated at different amplitudes and frequencies is presented in Figure 4.

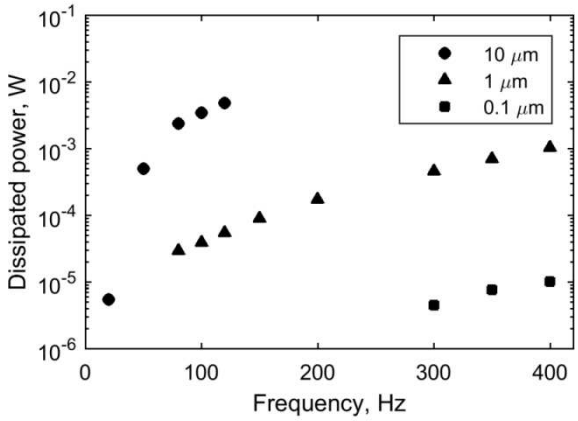

Figure 4: Measured power dissipation at different vibration amplitudes

As the dissipated power spans a very wide range of values, the final comparison between experiment and prediction was made using an equivalent viscous damper (that is, a grounded viscous damper that would dissipate power at an equivalent rate) so that results at different frequencies could be conveniently plotted on the same figure. The equivalent viscous damper is defined as,

$$c_{eq} = \frac{2P_{real}}{|V|^2} \tag{10}$$

4.3 Properties of equivalent solid

One of the parameters affecting the Young's modulus of the equivalent solid is the confining pressure: the relationship is described in Equation 7. The Janssen estimation for pressure using Equation 8 and properties defined in Table 2 for this container is shown in Figure 5. Uncertainty bounds of two standard deviations (approximately 95%) are also shown.

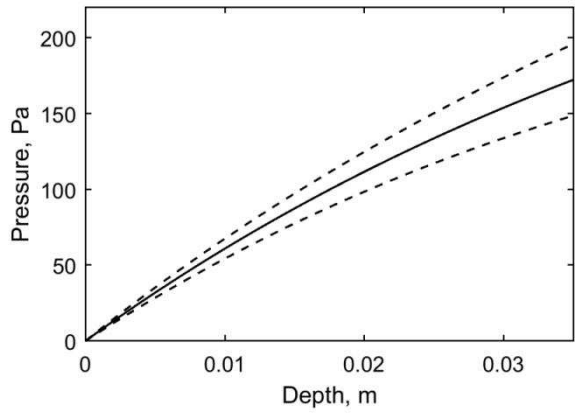

Figure 5: Pressure distribution in the box configuration (dashed lines show 2σ bound)

Examination of Figure 5 shows that even for a shallow container, the pressure is not purely hydrostatic – the high coefficient of friction results in some redistribution of the load to the container walls. Also,

in this experiment, the viscoelastic spheres were of significant size in comparison to the container depth resulting in a variation of true depth across the surface. Thus, considering Equations 7 and 8 together, the equivalent modulus of the granular medium varied throughout its volume and could vary depending on the exact arrangement of particles. As such a variation in depth and modulus was inconvenient for use with standard finite element analyses, the approach taken was to use properties at a depth of 18.7 mm – the mean depth obtained from the number of spheres and the fill ratio. Based on this approximation, an average pressure of 103.7 Pa and standard deviation 6.7 Pa were used in subsequent calculations.

The equivalent complex modulus for the granular fill, obtained using Equations 5 to 7 is shown in Figure 6. Note that the equivalent density had a mean value of 679 kg/m^3 and a standard deviation of 35 kg/m^3.

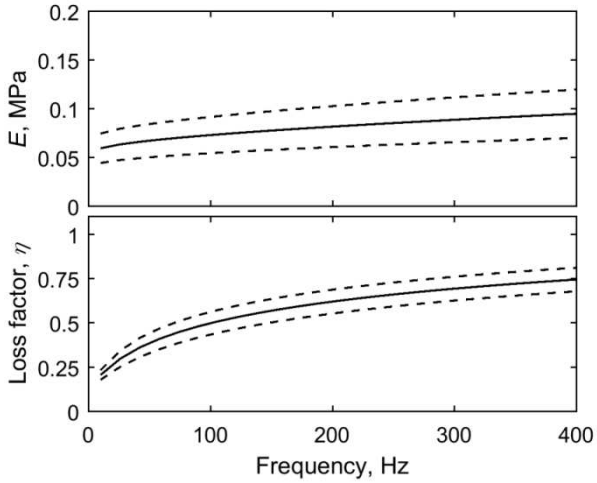

Figure 6: Equivalent properties of granular fill in the open-sided box (dashed lines show 2σ bounds)

4.4 Direct frequency response

With the complex modulus specified, one way to estimate the energy dissipation was to calculate the dissipated power when the system is subjected to sinusoidal base motion. To account for frequency dependence in the viscoelastic material, a Direct Frequency Response (DFR) calculation was performed on a finite element model of a block representing the equivalent viscoelastic material. The block was restrained on the five faces that would have contacted the inside of the box. Base motion was then prescribed at this boundary. The reaction force for displacement amplitude vector $\underline{\mathrm{X}}$ was,

$$\underline{\mathrm{F}} = \left[\mathbf{K}' + \mathrm{j}\mathbf{K}'' - \omega^2\mathbf{M}\right]\underline{\mathrm{X}} \tag{11}$$

where $\mathbf{K}'$, $\mathbf{K}''$ and $\mathbf{M}$ are the complex stiffness and mass matrices of the finite element model. The equivalent viscous damper was obtained from this information using Equations 9 and 10. Note that in the frequency domain $\underline{\mathrm{V}} = \mathrm{j}\omega\underline{\mathrm{X}}$.

The direct frequency response is computationally expensive as it requires the inversion of the impedance matrix for the full system at every desired frequency. Calculations were only attempted using the mean value for modulus rather than for all 1000 variations.

4.5 Modal approach

A procedure using properties of the vibration modes of the granular medium was also investigated. Normal eigenvalue analysis routines do not allow for frequency dependence of the modulus. As the finite element model involved a single material only – the equivalent solid – it was reasonable to assume that mode shapes were not affected by modulus and the natural frequencies varied according to,

$$\frac{\omega_{\mathrm{n}}}{\omega_{\mathrm{n,ref}}} = \sqrt{\frac{\mathrm{E}}{\mathrm{E}_{\mathrm{ref}}}} = \sqrt{\frac{\rho_{\mathrm{ref}}}{\rho}} \tag{12}$$

where $\omega_{\mathrm{n,ref}}$ is the natural frequency for a reference condition where the Young's modulus was $\mathrm{E}_{\mathrm{ref}}$ and the density ρ_{ref}. With this assumption, the vibration due to the base excitation of each mode could be summed. Hence, the force required to produce a given base motion amplitude X can be obtained for A modes using,

$$\mathrm{F} = \mathrm{X}\sum_{\mathrm{a}=1}^{\mathrm{A}} \mathrm{m}_{\mathrm{a}}\omega^2\left(\frac{1+\mathrm{j}2\zeta_{\mathrm{a}}\mathrm{r}_{\mathrm{a}}}{1-\mathrm{r}_{\mathrm{a}}^2+\mathrm{j}2\zeta_{\mathrm{a}}\mathrm{r}_{\mathrm{a}}}\right) \tag{13}$$

where m_{a} is the effective modal mass, r_{a} the ratio of the excitation frequency to the natural frequency of each mode and ζ_{a} the modal damping. Note that the modal damping in this case can be obtained from the material loss factor using,

$$\zeta_{\mathrm{a}} = \frac{\eta}{2} \tag{14}$$

In the work reported here, the first 1000 vibration modes of the block were found to span the desired frequency range 0 to 400 Hz. Because of Equations 12 and 14, only one eigenvalue extraction calculation was necessary. Subsequently, predictions were made for each of the 1000 variations in material property. Power and hence equivalent viscous damper values were then found.

4.6 Results

The equivalent dampers for experiment, DFR and modal methods are presented in Figure 7. It can be seen that the measured results at different amplitudes lie close to the predicted values. The DFR result

lies within the uncertainty bound of the modal method but it lies towards the lower boundary. The sudden rise in damping above approximately 60 Hz relates to the presence of the first wave mode in the granular material. Predictions above 400 Hz were not attempted as more modes would have been required from the eigenvalue extraction routine.

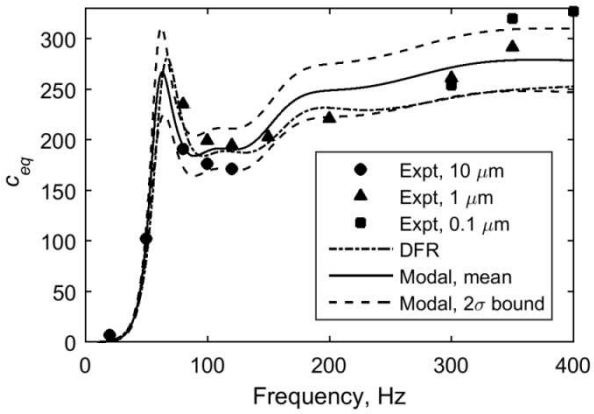

Figure 7: Equivalent damper for box subjected to horizontal excitation

Deformed shapes, from the DFR calculation, are presented in Figure 8 to show the increasing complexity of the standing waves as the frequency increases. It is interesting to note that significant vertical movement of the granular material occurs for this configuration.

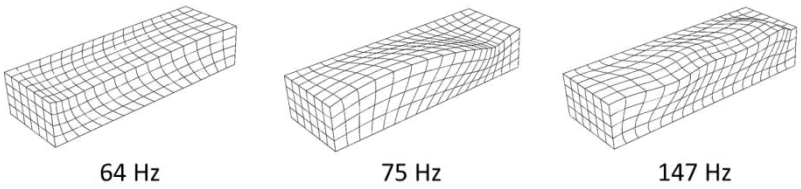

Figure 8: Section views of deformations within the granular medium at different frequencies

5 Composite tube assembly

In the previous section, it was shown that the equivalent solid model could be used in conjunction with standard finite element analysis to predict energy dissipation in granular materials subjected to low amplitude vibration. In this section, efforts are made to predict the frequency response of a typical engineering structure damped using a granular fill.

5.1 Composite tube assembly

This configuration involved a circular-section, roll-wrapped, carbon fibre composite tube fitted with heavy aluminium end caps. The tube was 1255 mm in length with an inner diameter of 50.7 mm and a

mean wall thickness of 1.8 mm. Push-fitting solid aluminium caps, whose dimensions are shown in Figure 9, were attached to the ends. The entire system was suspended vertically from the upper end cap while excitation was applied horizontally on the lower cap.

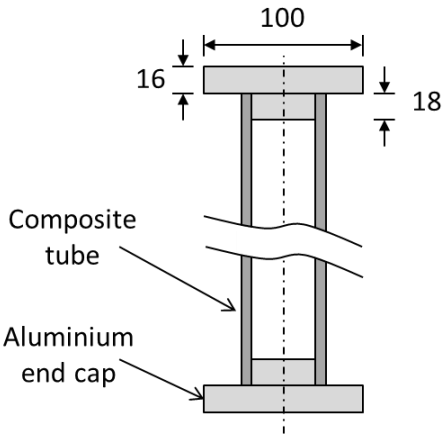

Figure 9: Composite tube assembly

Features of this configuration that made it interesting for this study include:

1. Non-parallel walls in the direction of forcing,
2. A deep cavity allowing for a significant build-up of static pressure within the granular medium,
3. A multi-part structure with different materials – specified in Table 3.

Table 3: Properties of composite tube assembly

Part	Property	Unit	Value
Tube	E (along tube)	GPa	85
	E (other directions)	GPa	19
	Shear modulus	GPa	4.6
	Poisson's ratio		0.14
	Density	kg/m^3	1600
End cap	E	GPa	70
	Density	kg/m^3	2700
	Poisson's ratio		0.33

This configuration was intended to provide suitably challenging conditions for the prediction methods to be tested under.

5.2 Experimental results

The composite tube assembly was suspended vertically using similar nylon line and helical springs as the box described in Section 3. As with the box, suspension modes were found to occur below 5 Hz. Vibration input was supplied by an electrodynamic exciter capable of delivering 100 N peak sine force. This was attached to the lower end cap in a radial direction through a force transducer. The response

was measured at both end caps at positions diametrically opposite the force transducer using miniature accelerometers.

Low amplitude, band-limited random excitation was applied to the structure and the acquisition system was set to obtain the frequency response function (FRF) based on 100 averages using a Hann window. For conciseness, results presented here focus on results obtained using the accelerometer attached to the same end cap as which forcing was applied. However, it was verified that measurements taken at the other end cap would have provided the same conclusions.

FRFs for the composite tube assembly empty and full of the granular material are presented in Figure 10. For the empty system, lightly damped resonances can be seen at 159, 492 and 921 Hz. When approximately 1.7 kg of spherical particles was used to fill the tube, the higher frequency resonances vanished while the damping ratio of the first resonance increased from 0.001 to 0.064. This level of fill, where the added mass of particles is approximately the same as the mass of the host structure, is not often practical for use. However, it was considered useful for this study as it provided an extreme case for the simulation methods to deal with.

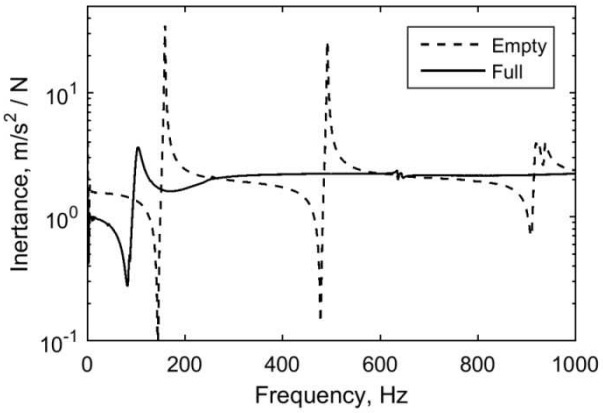

Figure 10: Measured frequency response of composite tube assembly

5.3 Predicted results

The frequency response of the tube was predicted using FE analysis and employing the equivalent solid assumption. Responses were calculated using both the DFR routine and a modal approach which is described below.

Material properties

The depth of the tube and the high coefficient of friction between particles meant that the pressure reached a limiting value at depths exceeding 0.1 metres – see Figure 11. Hence most of the granular material was at uniform pressure. For subsequent calculations therefore a nominal value of pressure was used for each simulation. This was defined as the average pressure through the volume after ignoring 5% of the fill lying nearest to the top surface.

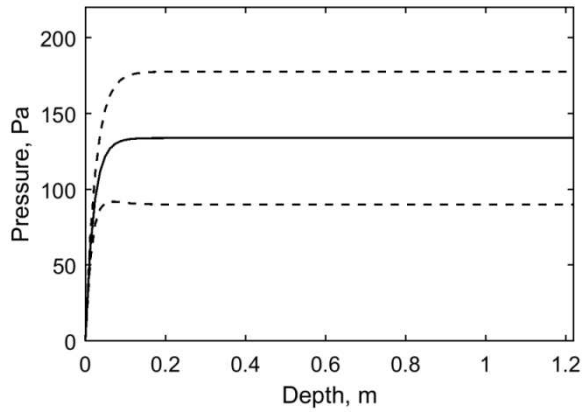

Figure 11: Pressure distribution in tube with depth (dashed lines show the 2σ bounds)

Complex modulus data were obtained for each of the 1000 variations of material properties using Equation 7. The mean and range of these properties with frequency is shown on Figure 12.

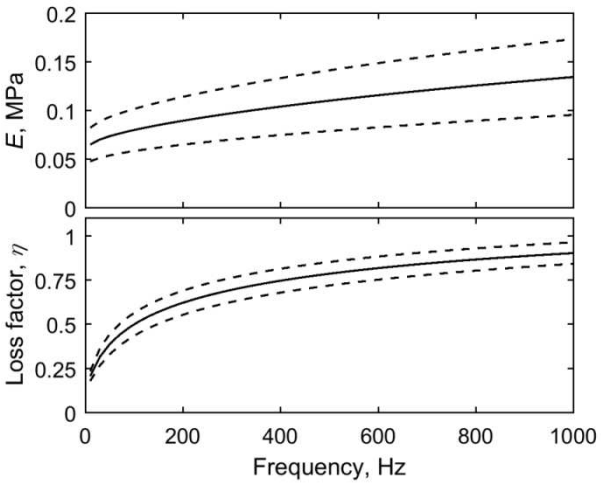

Figure 12: Equivalent properties of granular fill in the composite tube assembly (dashed lines show the 2σ bounds)

Response prediction

Because of computational expense, the DFR calculation was only carried out for one set of material properties – the average values. A modal approach was developed to allow faster evaluation of the results. Unlike the box discussed in the previous section, it was not possible to extract the vibration modes of a filled tube directly and adjust values according to exact modulus and density. This was because the size of the cavity meant that there were a very large number of wave modes in the granular medium: the 1500th vibration mode had a natural frequency below 300 Hz. Also, because the structure was made of several different materials, direct scaling would have been inaccurate. Instead, the

approach taken here involved combining analysis originally developed for thick, soft viscoelastic layers with FE based modal analysis of the empty structure.

Ungar and Kerwin (1964) were the first to show that vibration levels in a metal-viscoelastic structure can be reduced if standing waves are induced within the viscoelastic portion. They developed expressions for the energy stored and dissipated in a thick viscoelastic layer attached to a flat metal plate subjected to out-of-plane vibrations. Defining x and u to be the position and displacement perpendicular to the plate surface, they represented the motion within the layer using the wave equation,

$$\frac{d^2u}{dx^2} + k^2u = 0 \tag{15}$$

where at frequency ω, the complex wavenumber is,

$$k = k' + jk'' = \omega\left(\frac{\rho(1+\nu)(1-2\nu)}{E(1-\nu)}\right)^{\frac{1}{2}} \tag{16}$$

For a layer of thickness h_2 subjected to base plate motion of u_0, noting that the strain at the free surface is zero, they showed that the deflection in the layer is given by,

$$u = u_0\frac{\cos\left(kx - kh_2\right)}{\cos(kh_2)} \tag{17}$$

from which they derived expressions for peak kinetic energy and work done per cycle. These expressions were defined per unit area of the plate i.e. the area perpendicular to the direction of motion. Subsequently, House and Hilliar (1990) recognised that the deflection of material enclosed between face plates could be represented by the same equation because of symmetry, provided that h_2 was set as the distance from one wall to the centreline and the face plates did not move relative to one another. For these conditions, the average energy dissipation per radian is given by,

$$D = u_0^2\left(\frac{\rho\omega^2 h}{4}\frac{\eta}{\sqrt{1+\eta^2}}\frac{\frac{\sinh(k''h)}{k''h} - \frac{\sin(k'h)}{k'h}}{\cos^2\left(\frac{k'h}{2}\right) + \sinh^2\left(\frac{k''h}{2}\right)}\right) \tag{18}$$

where h the full depth of the granular medium in the direction of motion. In the same way, the peak kinetic energy in the granular medium is,

$$T = u_0^2\left(\frac{\rho\omega^2 h}{4}\frac{\frac{\sinh(k''h)}{k''h} + \frac{\sin(k'h)}{k'h}}{\cos^2\left(\frac{k'h}{2}\right) + \sinh^2\left(\frac{k''h}{2}\right)}\right) \tag{19}$$

While previous studies have generally focused on systems with parallel faces such as layered plates and box section beams, it is possible to approximate behaviour for cavities with non-parallel faces because the energy expressions are defined per unit area. Consider a segment depth h through the entire structure in line with the applied excitation which has area δ_s perpendicular to the excitation. If the walls at each end move by the same amount, Equations 18 and 19 can be applied to that segment. Summing over the entire area perpendicular to the excitation, the system loss factor can be defined as,

$$\eta = \frac{\text{energy dissipated per radian}}{\text{peak strain energy}} \approx \frac{\sum \mathrm{D}\delta_\mathrm{s}}{\sum \mathrm{T}\delta_\mathrm{s} + \mathrm{T_b}} \tag{20}$$

where $\mathrm{T_b}$ is the kinetic energy in the host structure.

In the most general case, the host structure is subject to resonant vibration. If the cavity is extensive, different parts may move by significantly different amounts. To keep the analysis simple, it was assumed in this work that the walls of the cavity directly opposite each other did not move relative to one another, effectively neglecting squashing or stretching of the cavity. The average motion of a unit segment of the cavity is therefore given as,

$$\mathrm{u_0} = \mathrm{q}^\mathrm{T}\psi \tag{21}$$

where ψ is the vector of average mode shapes of the cavity walls and q is the vector of coefficients describing the participation of individual modes in a particular vibration. Also, noting that at resonance the damping ratio is half the value of the loss factor, it can be expressed as,

$$\zeta \approx \frac{1}{2}\frac{\sum \mathrm{D}\delta_\mathrm{A}\psi_\mathrm{s}^2}{\sum \mathrm{T}\delta_\mathrm{s}\psi_\mathrm{s}^2 + \mathrm{T_b}\psi_\mathrm{b}^2} \tag{22}$$

where ψ_s is the specific mode shape at the cavity segment considered and ψ_b^2 is the average squared mode shape of the entire host structure.

In this way, it was possible to account for the damping from the granular material using the finite element model for the empty host structure. However, as the added mass of the granular material was significant, natural frequencies, modal masses and mode shapes of the host structure would have been changed considerably. In this work, to account for this, the mass of the granular fill was distributed evenly around the boundary of the cavity by increasing the density of the composite material to account for the added particles. The mass of the segment of composite tube encasing the particles was 0.579 kg. To account for the addition of 1.7 kg of particles, the density of these elements was raised to 6224 kg/m^3.

Within the frequency range of interest, the tube displayed three types of vibration mode: flexure (similar to a beam), torsion (with significant circumferential deflection) and modes where the tube walls bend.

Examples of these mode types are presented in Figure 13 while natural frequencies of the lower modes are presented in Table 4.

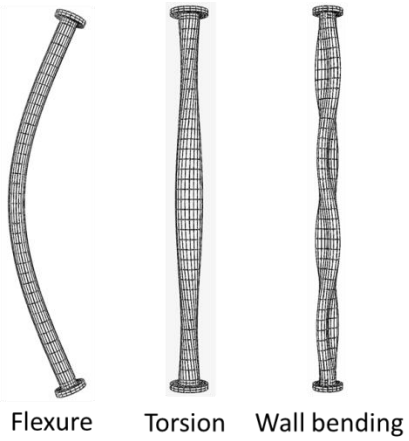

Figure 13: Mode types for the tube assembly

Table 4: Natural frequencies of the tube assembly

Mode Number	Mode type	Natural frequency, Hz	
		Empty	Full
1,2	Flexure	156	101
3	Torsion	272	227
4,5	Flexure	489	278
6	Torsion	797	494
7,8	Flexure	936	510
9,10	Tube wall	1164	590
11,12	Tube wall	1191	604
13,14	Tube wall	1259	638
15,16	Tube wall	1380	701
17,18	Flexure	1382	766

The frequency response was then calculated from the modal data using,

$$\frac{X}{F} = \sum_{a=1}^{A} \frac{\psi_{a,in}\psi_{a,out}}{m_a\left(\omega_{n,a}^2 - \omega^2 + j2\zeta_a\omega\omega_{n,a}\right)} \tag{23}$$

where m_a is the modal mass, $\psi_{a,in}$ and $\psi_{a,out}$ are the mode shape at forcing and measurement point respectively. Frequency responses for the 1000 variations in material properties calculated using this method can be seen in Figure 14. It can be seen that the scatter in the FRF was relatively low.

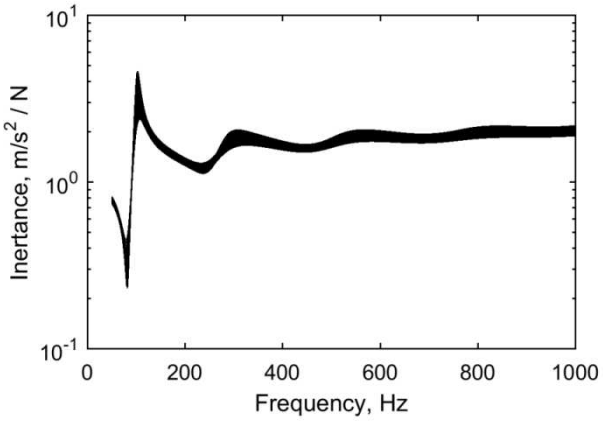

Figure 14: Predicted FRF curves modal data (all 1000 variations)

5.4 Comparison between measured and predicted behaviour

Frequency responses produced from the two numerical approaches are compared with the experimentally obtained response in Figure 15. For clarity, only the average modal response curve is shown on this plot.

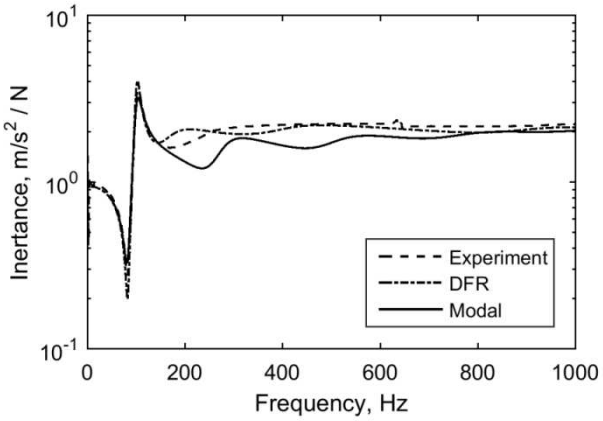

Figure 15: Comparison of FRF prediction methods against measured

It can be seen that all three curves lie relatively close to one another – particular if one considers the response before the granular fill was added (Figure 10). The DFR result is somewhat closer to the experiment. However, this is not wholly surprising considering the simplifications involved in the modal approach. Careful observation shows that the largest errors in the modal method occur at frequencies near the torsion modes (227 and 494 Hz) that involve significant deformation of the tube cross-section which makes the average motion assumption less accurate.

It is interesting to observe what is happening inside the granular medium as the tube vibrates. Cross sectional views of the tube at different frequencies are shown in Figure 16. Note that the excitation direction is parallel with the horizontal axis in this figure.

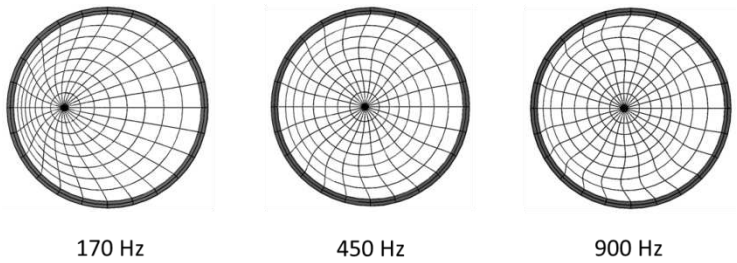

Figure 16: Section view of filled tube at different frequencies taken from DFR analysis

At low frequencies, the centre of the granular medium moves more or less in phase with the walls. As the frequency increases, the centre tends to deflect more than the walls and the phase difference increases. At 170 Hz, the frequency at which the loss factor is maximised according to Equation 20, the motion of the centre is 180° out of phase with the walls and of a similar magnitude. As the frequency increases further, the motion of the centre reduces towards zero and deformation of the granular fill involves higher order waves in the radial direction.

6 Limits of applicability

The work has shown that the prediction methods discussed in this work provide good estimates of energy dissipation and host structure vibration. For the box structure, it can be seen from Figure 7 that the prediction remains accurate for acceleration levels as high as 6 m/s^2. It was considered important to investigate the acceleration amplitude to which such methods are valid. The composite tube assembly was used for this experimental study.

The main difference between the testing done here and that reported in Section 5 was that amplitude-controlled sinusoidal forcing was used instead of random. As only the first resonance near 100 Hz was detectable, stepped-sine testing was concentrated around this frequency. Results for natural frequency and modal damping ratio are presented in Figures 17 and 18.

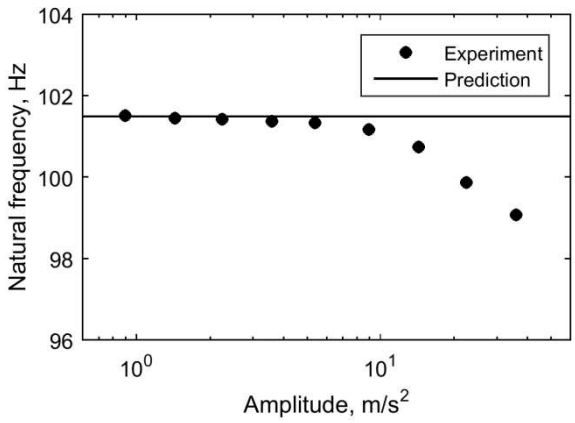

Figure 17: Natural frequency of first mode

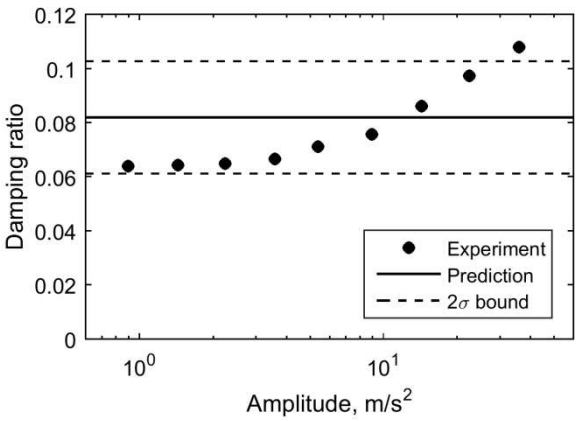

Figure 18: Damping ratio of first mode

It can be seen from the results that when the acceleration increases beyond approximately 4 m/s^2, results start to deviate from the prediction: natural frequencies drop at higher amplitudes and damping ratios increase due to the added contribution of friction at the interfaces. For this mode, vibration at the tube midpoint is around 16% higher than at the measurement point. Also, from Equation 17, it can be found that the ratio of the motion at the centre of the fill to the tube wall is approximately 2.2. The condition under which the equivalent solid approximation begins to fail is therefore approximately the point at which the largest motion in the bulk of the granular material exceeds gravity. This is consistent with the findings of Poschel et al (2000).

7 Conclusions

This paper set out to develop and evaluate prediction methods for viscoelastic granular dampers under low amplitude vibrations that are compatible with commercial finite element analysis software and can be used for irregular cavities. The work has demonstrated two methods that achieve this to reasonable accuracy. Both rely on modelling the medium as a solid and on obtaining equivalent elastic properties. One method uses the Direct Frequency Response and although computationally expensive, will provide reliable predictions. The other approach involves combining standard eigenvalue-based mode extraction routines with theoretical approximations that yield modal damping ratios. This approach is inexpensive in terms of computing effort.

The effectiveness of these methods was demonstrated by comparing predictions with experimental results from two very different experimental configurations. An rigid open box was used to study the energy dissipation over a range of frequencies. This showed that dissipation increased once standing waves were generated in the granular medium. A composite tube with heavy metallic ends was used to show the effectiveness of the methods in the predicting frequency response of a structure damped using viscoelastic granules. In both cases, the predictions matched the measured results with reasonable accuracy.

A numerical study showed that while the arrangement of the granular system could vary significantly, the overall effect on the energy dissipation and damping were not dramatic. Experiments also showed that for the particles considered, equivalent solid type behaviour was observed up to approximately the acceleration due to gravity. Damping tended to increase as the amplitude rose beyond this. This result shows that in this type of granular system, energy is dissipated primarily within the particles at low amplitudes however frictional losses become significant when the bulk acceleration levels within the granular medium approach that of gravity.

References

Ben-Haim Y (2001) Information-Gap Theory: Decisions under severe uncertainty. Academic Press, London.

Darabi B and Rongong JA (2012) Polymeric particle dampers under steady-state vibrations. Journal of Sound and Vibration, 313, 3304-3316.

Ferry JD (1980) Viscoelastic properties of polymers. John Wiley & Sons.

House JR and Hilliar AE (1990) Vibration Damping Materials. WIPO International Patent Classification F16F7/00, G10K11/16. International Publication Number WO90/01645.

Iwata H and Homma T (1974) Distribution of coordination numbers in random packing of homogeneous spheres. Powder Technology, 10, 79-83.

Janssen HA (1895) Experiments on grain pressure in silos. Transactions of the Association of German Engineers, 39, 1045–1049.

Nolan GT and Kavanagh PE (1992) Computer simulation of random packing of hard spheres, Powder Technology, 72, 149-155.

Oyadiji SO (1996) Damping of vibration of hollow beams using viscoelastic spheres. Proceedings of Smart Structures and Materials: Damping and Isolation, San Diego, SPIE Vol. 2720, 89-98.

Pamley RJ, House JR and Brennan MJ (2001) Comparison of passive damping treatments for hollow structures. Proceedings of Smart Structures and Materials: Damping and Isolation, Newport Beach, SPIE Vol. 4331, 455-467.

Rongong JA, Tomlinson GR (2002) Vibration damping using granular viscoelastic materials. Proceeding of ISMA 27, Noise and Vibration Engineering Conference, Leuven, Belgium, 431-440.

Ungar EE and Kerwin EM (1964) Plate damping due to thickness deformations in attached viscoelastic layers. Journal of the Acoustical Society of America, 36(2), 384-392.

Varanasi KK and Nayfeh SA (2006) Damping of flexural vibration using low-density, low-wave-speed media. Journal of Sound and Vibration, 292, 402–414.

Poschel T, Schwager T and Saluena C (2000) Onset of fluidization in vertically shaken granular material, Physical Review E, 62 (1), 1361-1367.

Walton K (1987) The effective elastic moduli of a random packing of spheres. Journal of the Mechanics and Physics of Solids, 35 213-26.

Zamponi F (2008) Packing close and loose, Nature, 453, 606-607.